

A FREWARE PROGRAM FOR PRECISE OPTICAL ANALYSIS OF THE FRONT SURFACE OF A SOLAR CELL

Simeon C. Baker-Finch and Keith R. McIntosh

Centre for Sustainable Energy Systems, Australian National University, Canberra, ACT 0200, AUSTRALIA
Tel: +61-2-6125-8966, Fax: +61-2-6125-8873, Email: simeon.bakerfinch@gmail.com, krmcintosh@gmail.com

ABSTRACT

This paper describes a freeware program that computes the optical losses associated with the front surface of a silicon solar cell. The optical losses are not trivial to assess because (i) the refractive index and extinction coefficient of silicon, antireflection coatings (ARCs), and encapsulants varies with wavelength; (ii) cells are usually textured such that the light reflects multiple times from the front surface; (iii) light can be polarised, particularly after the first 'bounce' from a textured surface; and (iv) the incident spectrum and the cell's quantum efficiency varies with wavelength. The freeware program takes all of these aspects into account to calculate reflection from the solar cell, absorption in the ARCs, transmission into the silicon, and the equivalent current that is generated for any given spectrum. When modelling textured silicon, the program is restricted to normally incident light and pyramidal morphologies. The program computes solutions within one second for regular upright pyramids, regular inverted pyramids, and random upright pyramids—making it much faster than ray tracing. We provide an example of how the freeware can be employed to determine the optimal thickness of an ARC with and without encapsulation. The example demonstrates that the optimal thickness cannot be determined from reflection measurements when absorption in the ARCs is significant. The program is readily adaptable to assess ARCs on glass and thin-film solar cells.

INTRODUCTION

The combination of surface texturing and antireflection coatings (ARCs) greatly enhances the ability of a solar cell to absorb the incident radiation. However, these features tend to complicate the assessment of the associated optics.

Firstly, an ARC introduces interference, and therefore the reflection, absorption and transmission by the ARC depends on its thickness, its refractive index $n(\lambda)$ and its extinction coefficient $k(\lambda)$. Moreover, the interference depends on $n(\lambda)$ of the overlying layer (often EVA for an encapsulated solar cell) and $n(\lambda)$ and $k(\lambda)$ of the underlying active semiconductor (such as silicon). Complicating matters further, both $n(\lambda)$ and $k(\lambda)$ can vary significantly with wavelength λ , and the interference depends on the angle and polarisation of the incident light.

Secondly, the surface texturing causes light to reflect multiple times from the front surface. Thus, the reflection, absorption and transmission by the ARC must be calculated for each 'bounce' of light, and combined correctly to determine the net reflection, absorption and transmission. It is clearly necessary to determine how the texture alters the angle of incidence and the polarisation of the light. (The latter is often ignored but is significant for inverted pyramids and random upright pyramids. Often, double bounce reflection in opposite pyramid facets is the only case considered [1, 2].)

These complex optical structures can be solved via geometrical ray tracing (as long as features are large enough to render diffractive effects negligible). However, ray tracing programs can be computationally time consuming, and not all freely available ray tracers account for a non-zero extinction coefficient or polarisation.

We present a freeware computer program that, assuming normal incidence, accurately models the multiple bounce interaction of light ray and surface texture, accounts for wavelength-dependent complex refractive indices, and implements a rigorous approach to the analysis of the polarisation of the ray as it interacts with the structure [3]. The program can be used to accurately calculate wavelength-dependent reflectance, ARC absorptance, and transmittance for a range of common solar cell surface morphologies.

In addition, the program calculates the resulting generation current J_{gen} within the cell substrate. It therefore permits the optimisation of an ARC that maximises J_{gen} .

In this paper, we first describe the general approach taken by the freeware program. We then present an example of its application to the calculation of the thickness of an antireflection coating of known refractive index by matching measured data. In a second application, we show that the program can be employed to optimise the thickness of an ARC with and without encapsulation. The program can be attained by contacting either author.

MAJOR INPUTS AND OUTPUTS

The user first selects the following:

- a superstrate material, such as air, EVA or silicone;
- an ARC material, such SiN_x, TiO₂, ZnO, or SiO₂, and its thickness;

- a substrate material, such as silicon or glass;
- a surface texture morphology amongst a choice of planar, regular upright pyramids, regular inverted pyramids or random upright pyramids.

In fact, the user can institute any number of ARC layers, and any material in place of the common materials available in the drop-down lists, provided they have suitable data for $n(\lambda)$ and $k(\lambda)$. We also note that $n(\lambda)$ and $k(\lambda)$ of many materials can vary substantially, depending on process conditions— SiN_x is a good example (see Refs. [4] and [5]).

Given $n(\lambda)$, $k(\lambda)$ and the thickness of the materials, the program calculates:

- wavelength-dependent front surface reflectance,
- wavelength-dependent absorptance of the ARC, and
- wavelength-dependent transmittance of the front surface (proportion of light transmitted into the substrate).

Coupling the calculation of front surface transmittance with a user-defined incident spectrum and light trapping parameters, the program calculates the electrical current absorbed in the substrate; this process is described in more detail below.

COMPUTATIONAL APPROACH

In the following discussion, we describe the computational approach used in the program by way of an example. In particular, we examine the front surface of a crystalline silicon solar cell textured with a regular array of upright pyramids and coated with a 60 nm thick amorphous SiN_x layer. The real and imaginary refractive indices used for silicon, SiN_x , and EVA are given in [6], [3] and [7], respectively.

(a) Ray paths

Every ray that is incident to a given morphology follows just one of a certain number of possible paths. For example, in the case of regular upright pyramids, all normally incident rays intersect a pyramid facet at 54.74° and then an opposing facet at 15.79° , but just 11.1% of those rays intersect the first facet again at 86.32° [3]. Thus, there are two possible paths: 88.9% of incident rays suffer two bounces and 11.1% suffer three bounces.

In the case of regular inverted pyramids, there are three possible paths, and in the case of random upright pyramids there are seven possible paths, for normally incident light. The additional paths correspond to rays that glance from facets that are perpendicularly aligned to the initial facet. For the regular pyramidal textures, the fraction of rays that follow a given path can be determined geometrically, whereas for the random pyramidal textures, the fraction is best determined by ray tracing. We have presented those fractions in [3]. (In the case of a planar morphology, there is, of course, just one possible path for any angle of incidence.)

Importantly, the fraction of rays that follows a given path is independent of the reflection and absorption at

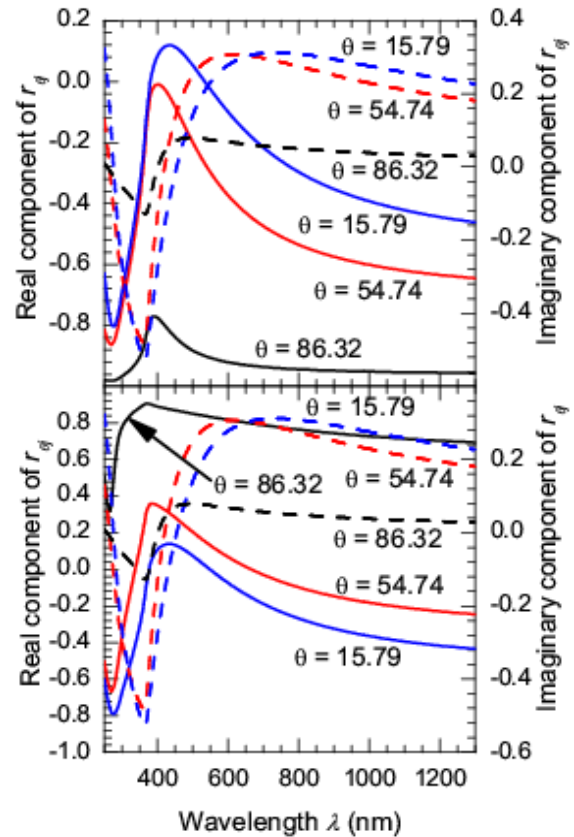


Figure 1: The real and imaginary components of the complex amplitude reflection coefficients for TE (top) and TM (bottom) waves arriving at the various angles of incidence relevant to a texture consisting of regular upright pyramids. Imaginary components are displayed as dashed lines.

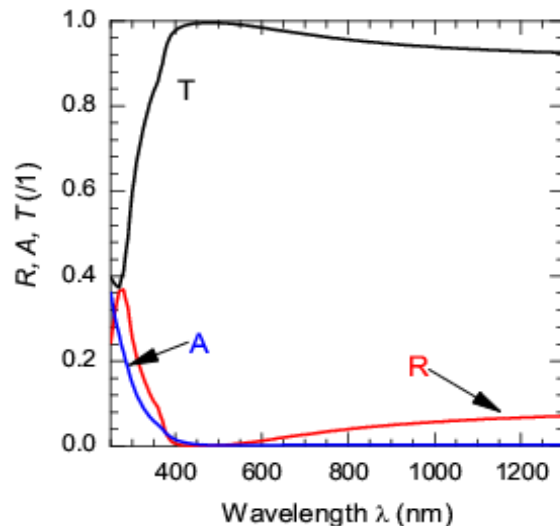


Figure 2: Wavelength-dependent reflectance, absorptance and transmittance of a SiN_x -coated, pyramidally-textured c-Si surface.

each bounce. Consequently, one can determine the net reflectance, absorption and transmittance associated with a given texture by determining the reflectance, absorption and transmittance at just a few known angles of incidence and combining them appropriately [3].

(b) Calculating reflectance, ARC absorptance, and transmittance

First, the amplitude reflection and transmission coefficients for p- (TM) and s-oriented (TM) waves, $r_{p,\theta}$, $r_{s,\theta}$, $t_{p,\theta}$, and $t_{s,\theta}$ are determined for the series of relevant angles of incidence, θ_j . These coefficients are determined for thin-film stacks via an adaptation of the matrix method described by Macleod [8]. Their values are shown in Figure 1.

Once calculated, the coefficients are used to populate the so-called Jones' matrix. Thereafter, a rigorous polarisation ray tracing calculus (as described by Yun *et al.* [9] and applied to solar cells in our previous work [3]) is used to determine the reflectance, transmittance and ARC absorptance along various reflection paths. This approach is required for inverted pyramids and random pyramids due to some rays glancing from facets that are perpendicular to the initial facet of incidence. For brevity, the associated equations are not included here, but it is not required of regular upright pyramids morphology (though for consistency, the program goes through the process regardless). Instead, the total wavelength-dependent front surface reflectance from regular upright pyramids is given by

$$R_{reg,up} = 0.8889R_A + 0.1111R_B, \quad (1)$$

where

$$R_A = \frac{R_{p,54.74^\circ} R_{p,15.79^\circ} + R_{s,54.74^\circ} R_{s,15.79^\circ}}{2}, \quad (2)$$

$$R_B = \frac{R_{p,54.74^\circ} R_{p,15.79^\circ} R_{p,86.32^\circ} + R_{s,54.74^\circ} R_{s,15.79^\circ} R_{s,86.32^\circ}}{2}, \quad (3)$$

$$R_{p/s,\theta} = r_{p,\theta_j} r_{p,\theta_j}^*, \quad (4)$$

and * denotes the complex conjugate. The total reflectance and absorptance are calculated via similar equations, and are shown in Figure 2.

(c) Evaluating generation current and sources of loss

The generation current density, J_{gen} , which represents the photon current absorbed in the active region, is equivalent to the short circuit current density when the collection efficiency $\eta_c(\lambda) = 1$. It is given by

$$J_{gen} = \int_{\lambda} I(\lambda) \cdot [1 - R(\lambda) - A(\lambda)] \cdot \{1 - \exp(-Z(\lambda)W\alpha(\lambda))\} \cdot d\lambda. \quad (5)$$

where Z is the pathlength enhancement that arises from internal reflections in the cell and W is the width of the cell.

With user-defined values for W and $Z(\lambda)$ (options in the current program include setting $Z(\lambda)$ to be constant with λ or at its ideal upper limit of $Z = 4n(\lambda)^2$, where n is the real

part of the refractive index of the absorber), the program calculates J_{gen} , as well as losses associated with front surface reflection and absorption ($J_{loss,R}$ and $J_{loss,A}$, respectively) according to

$$J_{loss,R} = \int_{\lambda} I(\lambda) \cdot R(\lambda) \cdot \{1 - \exp(-Z(\lambda)W\alpha(\lambda))\} \cdot d\lambda, \quad (6a)$$

$$J_{loss,A} = \int_{\lambda} I(\lambda) \cdot A(\lambda) \cdot \{1 - \exp(-Z(\lambda)W\alpha(\lambda))\} \cdot d\lambda. \quad (6b)$$

Note that the incident flux $I(\lambda)$ is chosen from a set of predefined spectra.

The outputs for this example are $J_{gen} = 40.93 \text{ mA/cm}^2$, $J_{loss,R} = 1.33 \text{ mA/cm}^2$ and $J_{loss,A} = 0.23 \text{ mA/cm}^2$. For the simulation, we chose an AM 1.5-G incident spectra, and approximated a high-efficiency silicon solar cell by choosing a substrate width of $W = 200 \text{ }\mu\text{m}$ and a pathlength enhancement of $Z = 6$.

DETERMINATION OF EXPERIMENTAL ARC THICKNESS

The program provides a simple and accurate tool for determining the thickness of a single-layer ARC from a given diffuse reflectance curve. An example of such a curve was measured with a Varian Cary 5000 Spectrophotometer with integrating sphere, and is shown in Figure 3. (The escape reflection has been removed from the curve so that just the front surface reflection can also be plotted). The crystalline silicon sample was textured with random upright pyramids and coated with a thermal oxide. An oxide thickness of 100 nm was approximated based on the process time.

The oxide thickness input in the freeware program was varied, and a range of possible reflectance curves were generated for the sample structure. The best fit to the oxide thickness (107 nm) was chosen based on the minimization of the least squares error. The simulated curve closely matches the measured data.

It is emphasised that the accuracy of the calculated ARC thickness depends critically on the use of accurate $n(\lambda)$ and $k(\lambda)$ for the ARC. These values are well characterised and vary little for the thermal oxide of the example above, though this is not the case for many other ARC materials.

OPTIMISATION OF ARC THICKNESS

The thickness of an ARC layer can be optimised by maximising J_{gen} . The program provides the facility to calculate this optimal thickness. In Figure 4, J_{gen} is plotted as a function of SiN_x thickness for an example structure: crystalline silicon is textured with regular inverted pyramids and confined to have a 20 nm thick passivating silicon dioxide. Values of $I(\lambda)$, Z and W are those used in the previous example. In case (a), the superstrate is air and in case (b) it is EVA. Note that the reflection from module glass and EVA absorption are not considered in the second optimisation.

Figure 4 confirms the importance of considering absorption in an ARC. Were the thickness optimisation to be based on the minimisation of front surface reflection, the optimal thickness would be overestimated: the minima of the $J_{loss,R}$ curves do not coincide with the maxima of the J_{gen} curves (marked by the stars). Note that the optimal ARC thickness depends strongly on $n(\lambda)$ and $k(\lambda)$, which can vary significantly for SiN_x depending on the deposition and annealing/firing conditions.

INTERNAL REFLECTION

The examples thus far have concerned the external reflection of incident light. The program can also assess internal reflection—though still restricted to normally incident rays for pyramidal textures. For example, for an unencapsulated silicon cell, one can set the substrate to silicon and the superstrate to air. The resulting reflection represents the internal reflection of the cell.

CONCLUSION

The freeware program described here offers a rapid and accurate means to analyse the complicated optics at the solar cell front surface. The program takes into account the possibility that surfaces may be textured and coated with materials of complex refractive indices. It correctly deals with polarisation. Optical losses are easily identified via the calculation of a generation current density.

ACKNOWLEDGEMENTS

We are grateful to David Smith from SunPower Corporation for introducing us to the idea of calculating reflection from textured cells using a generalised path analysis.

REFERENCES

- [1] S. C. Chiao J. L. Zhou and H. A. Macleod, *Appl. Optics* **32** (28) 5557-5560 (1993).
- [2] J. Zhao and M. A. Green, *IEEE. Trans. Electron Dev.* **38** (8) 1925-1934 (1991).
- [3] S. C. Baker-Finch and K. R. McIntosh, submitted to *Prog. Photovoltaics*.
- [4] J. Hong *et al. J. Vac. Sci. Technol. B* 21 (5) 2123-2132 (2003).
- [5] W. Soppe, H. Rieffe and A. Weeber, *Prog. Photovoltaics* 13 : 551-569 (2005)
- [6] M. A. Green and M. J. Keevers, *Prog. Photovoltaics* **3** (3), 189-192 (2007).
- [7] K.R. McIntosh, J.N. Cotsell, J.S. Cumpston, A.W. Norris, N.E. Powell and B.M. Ketola, *Proc. 34th IEEE PVSC*, Philadelphia, pp. 544–549, 2009.
- [8] H. A. Macleod, *Thin Film Optical Filters*, ch. 2 (2001).
- [9] G. Yun, K. Crabtree and R. Chipman, *Proc. SPIE v. 6682 (Polarisation Science and Remote Sensing III)*, 66820Z (2007).

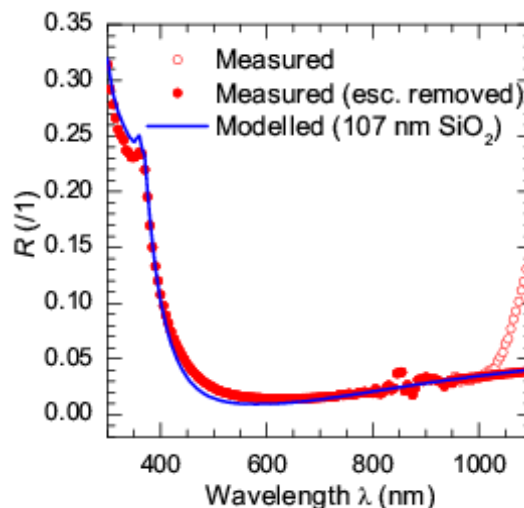


Figure 3: Measured and modelled reflectance curves for a silicon wafer textured with random upright pyramidal texture and coated with a thermal SiO_2 . (Best viewed in colour).

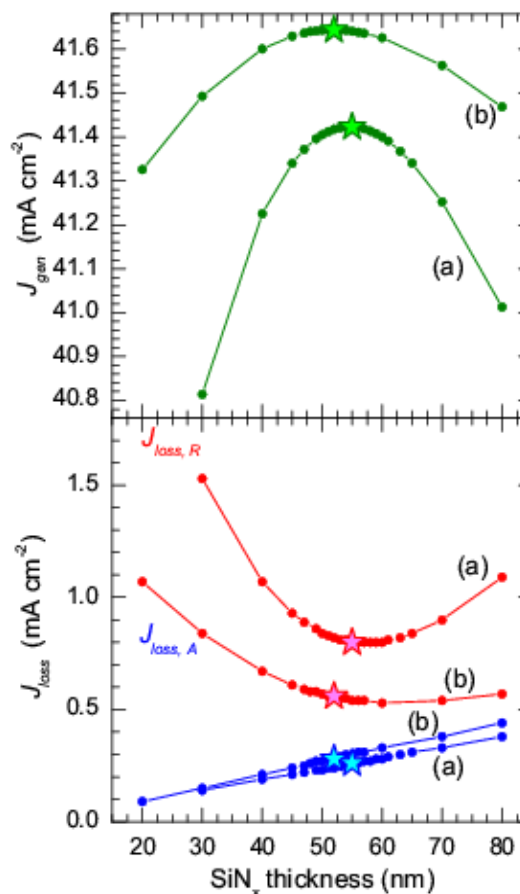


Figure 4: Generation current (top) and optical losses (bottom) as a function of SiN_x thickness for the structure described in the text, with (a) air and (b) EVA as the superstrate. The optimal SiN_x thickness is marked by a star on each curve.